Hindawi
Journal of Sensors
Volume 2024, Article ID 4574372, 8 pages
https://doi.org/10.1155/2024/4574372

Research Article

Hybrid RSS–AOA-Based Localization with Unknown Transmit Power in Wireless Sensor Networks

Ruijie Ren,[1] Jianding Yu,[1] Youming Li ,[1] Qinke Qi,[1] and Yanhua Ye [2]

[1]*Faculty of Electrical Engineering and Computer Science, Ningbo University, Ningbo 315211, China*
[2]*China Mobile Group Zhejiang Co, Ltd., Ningbo Branch, Ningbo, China*

Correspondence should be addressed to Youming Li; liyouming@nbu.edu.cn

Received 5 December 2022; Revised 13 May 2023; Accepted 15 December 2023; Published 24 January 2024

Academic Editor: Huan Liu

In this paper, we address the target localization problem based on hybrid range and angle measurements with unknown transmit power in both noncooperative and cooperative scenarios, respectively. By analyzing the approximate expressions of the noise terms in the measurement models, an original nonconvex localization problem is formulated according to the least square criterion. This problem is transformed into a mixed semi-definite programing/second-order cone programing by using convex relaxation techniques. Computer simulation results verify that the proposed algorithm can effectively solve the localization problem with good performance in the unknown transmit power case.

1. Introduction

Nowadays, target location has been an increasingly important information due to its wide applications in navigation, tracking, monitoring, etc. [1]. However, the global positioning system (GPS) cannot provide accurate location information in indoor or other harsh environments due to the disability of GPS signals to penetrate in-building materials [2, 3]. Wireless sensor networks attract more attention as they can provide localization information in such harsh environments. Based on the localization measurements related to distance, the methods can be divided into time of arrival (TOA) [4, 5], time difference of arrival (TDOA) [6], received signal strength (RSS) [7–9], angle of arrival (AOA) [9, 10], and their combination [11–13]. Compared with TDOA and TOA, the RSS-based localization method is attractive due to its low cost and easy tractability, and does not cause substantial power consumption. However, the performance of the single measurement localization method is limited, especially because the accurate model parameters, including transmit power and path loss exponent, are difficult to be determined in the actual environment. Currently, many methods based on hybrid RSS–AOA measurements have been proposed to improve the performance [14–17]. In the case of noncooperative localization, Yu [14] proposed a WLS estimator based on hybrid RSS–AOA measurements when the transmit power is known and provided a closed-form solution without considering any constraint conditions, causing low estimation accuracy. Qi et al. [15] proposed a WLS estimator when the transmit power is known, which is converted into RLS-semi-definite programing (SDP) problem by using the semi-definite relaxation (SDR) technique. The authors also extended the results to the case when the transmit power is unknown. In the case of cooperative localization, Tomic et al. [16] studied the localization problem when the transmit power is known. They fuzed RSS and AOA measurements by using spherical characteristics, proposed a least square (LS) estimator through a linearized measurement model, and provided a closed-form solution. Tomic et al. [17] also studied the problem when the transmit power is unknown and formulated an original LS problem, which is transformed into an SDP problem by using SDR technology.

In this paper, we address the noncooperative and cooperative hybrid RSS–AOA-based localization problem with unknown transmit power. We jointly estimate the target location and transmit power through the following three steps. First, we derive the approximation expressions of noise terms using first-order Taylor expansion for measurement models. Next, we formulate a nonconvex localization problem based

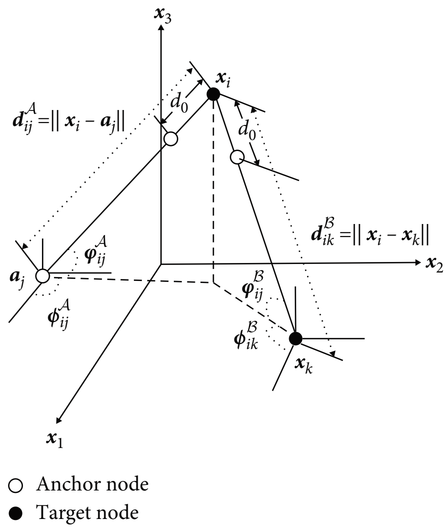

Figure 1: Localization scenario.

on the LS criterion. Finally, we transform the nonconvex problems into convex ones by introducing some auxiliary variables and using some relaxation techniques.

Notation: In this paper, uppercase bold letters and lowercase bold letters, respectively, denote matrices and vectors, lowercase regular letters denote scalars. $\|\cdot\|$ denotes the norm of a vector, $(\cdot)^T$ denotes the transpose of a vector or matrix, $\boldsymbol{I}_N$ denotes N dimensional identity matrix, $\mathbb{R}^N$ denotes N dimensional vector, matrix $\boldsymbol{A} \succeq \boldsymbol{B}$ denotes that matrix $\boldsymbol{A} - \boldsymbol{B}$ is a semi-definite matrix.

The reminder of the paper is arranged as follows: Section 2 describes the localization model and the derivation of the algorithm in detail, Section 3 analyses the computational complexity of the proposed and other discussed algorithms, Section 4 discusses Cramer–Rao Lower Bound (CRLB) of the proposed algorithm, Section 5 shows simulation results and analyze in detail.

2. Problem Formulation

A sensor network consists of M targets with unknown locations $\boldsymbol{x}_1, \boldsymbol{x}_2, \ldots, \boldsymbol{x}_M$ and N anchors with known locations $\boldsymbol{a}_1, \boldsymbol{a}_2, \ldots, \boldsymbol{a}_N$ in a 3D localization scenario, as shown in Figure 1.

Let $A = \{(i,j) | \|x_i - a_j\| \leq R\}$ and $B = \{(i,k) | \|x_i - x_k\| \leq R\}$ denote target/anchor and target/target communication links, respectively, where R denotes effective communication range of sensors.

In this paper, hybrid range and angle measurements are utilized to model our localization problem.

First, RSS measurement can be modeled by using path loss model, the relationship between RSS measurement and path loss is $L_{ij}(dB) = 10\log_{10}(P_T/P_{ij})$, where P_T denotes transmit power, L_{ij} and P_{ij} denote path loss value and receive power between the two nodes i and j, respectively. Then, the RSS measurement can be modeled as follows:

$$L_{ij}^A = L_0 + 10\gamma \log_{10}\left(\frac{\|\boldsymbol{x}_i - \boldsymbol{a}_j\|}{d_0}\right) + n_{ij}\ (i,j \in A), \tag{1}$$

$$L_{ik}^B = L_0 + 10\gamma \log_{10}\left(\frac{\|\boldsymbol{x}_i - \boldsymbol{x}_k\|}{d_0}\right) + n_{ik}\ (i,k \in B), \tag{2}$$

where d_0 denotes the reference distance, L_0 denotes the reference path loss value at d_0, γ denotes path loss exponent, $\|\boldsymbol{x}_i - \boldsymbol{a}_j\|$ and $\|\boldsymbol{x}_i - \boldsymbol{x}_k\|$ denote the real distance between anchor/target and target/target, respectively, RSS measurement noises n_{ij} and n_{ik} can be modeled as $n_{ij} \sim N(0, \sigma_{n_{ij}}^2)$ and $n_{ik} \sim N(0, \sigma_{n_{ik}}^2)$, respectively.

Second, according to the geometric relationship, the AOA azimuth and elevation measurements can be modeled, respectively, as follows:

$$\phi_{ij}^A = \arctan\left(\frac{\boldsymbol{x}_{i2} - \boldsymbol{a}_{j2}}{\boldsymbol{x}_{i1} - \boldsymbol{a}_{j1}}\right) + m_{ij}\ (i,j) \in A, \tag{3}$$

$$\phi_{ik}^B = \arctan\left(\frac{\boldsymbol{x}_{i2} - \boldsymbol{x}_{k2}}{\boldsymbol{x}_{i1} - \boldsymbol{x}_{k1}}\right) + m_{ik}\ (i,k) \in B, \tag{4}$$

$$\varphi_{ij}^A = \arccos\left(\frac{\boldsymbol{x}_{i3} - \boldsymbol{a}_{j3}}{\|\boldsymbol{x}_i - \boldsymbol{a}_j\|}\right) + v_{ij}\ (i,j) \in A, \tag{5}$$

$$\varphi_{ij}^B = \arccos\left(\frac{\boldsymbol{x}_{i3} - \boldsymbol{x}_{k3}}{\|\boldsymbol{x}_i - \boldsymbol{x}_k\|}\right) + v_{ik}\ (i,k) \in B, \tag{6}$$

where the azimuth and elevation measurement noises m_{ij}, m_{ik} and v_{ij}, v_{ik} are also modeled as $m_{ij} \sim N(0, \sigma_{m_{ij}}^2)$, $m_{ik} \sim N(0, \sigma_{m_{ik}}^2)$ and $v_{ij} \sim N(0, \sigma_{v_{ij}}^2)$, $v_{ik} \sim N(0, \sigma_{v_{ik}}^2)$.

Next, we perform first-order Taylor expansion and omit the second-order and above noise terms when the noise is small.

In this case, the expressions of noise terms of (1)–(6) have the following approximations:

$$n_{ij} \approx \frac{\mu^{-1}\left(\eta d_0^2 - \left(\beta_{ij}^A\right)^2 \|\boldsymbol{x}_i - \boldsymbol{a}_j\|^2\right)}{2\eta}, \tag{7}$$

$$n_{ik} \approx \frac{\mu^{-1}\left(\eta d_0^2 - \left(\beta_{ik}^B\right)^2 \|\boldsymbol{x}_i - \boldsymbol{x}_k\|^2\right)}{2\eta}, \tag{8}$$

$$\xi_{ij}^A \approx \boldsymbol{c}_{ij}^T(\boldsymbol{x}_i - \boldsymbol{a}_j), \tag{9}$$

$$\xi_{ik}^B \approx \boldsymbol{c}_{ik}^T(\boldsymbol{x}_i - \boldsymbol{x}_k), \tag{10}$$

$$\boldsymbol{k}^T(\boldsymbol{x}_i - \boldsymbol{a}_j) = \|\boldsymbol{x}_i - \boldsymbol{a}_j\| \cos\varphi_{ij}^A + \zeta_{ij}^A, \tag{11}$$

$$\boldsymbol{k}^T(\boldsymbol{x}_i - \boldsymbol{x}_k) = \|\boldsymbol{x}_i - \boldsymbol{x}_k\| \cos\varphi_{ik}^B + \zeta_{ik}^B, \tag{12}$$

where $\eta=\eta_0^2$, $\eta_0=10^{\frac{-L_0}{10\gamma}}$, $\mu=d_0^2\frac{\ln 10}{10\gamma}$, $10^{\frac{-n_i}{10\gamma}}\approx 1-\frac{\ln 10}{10\gamma}n_i$, $\beta_{ij}^A=10^{\frac{-L_{ij}^A}{10\gamma}}$, $\beta_{ik}^B=10^{\frac{-L_{ik}^B}{10\gamma}}$, $\boldsymbol{c}_{ij}=[-\sin(\phi_{ij}^A),\ \cos(\phi_{ij}^A),\ 0]^T$, $\boldsymbol{c}_{ik}=[-\sin(\phi_{ik}^B),\ \cos(\phi_{ik}^B),\ 0]^T$, $\boldsymbol{k}=[0,\ 0,\ 1]^T$.

The expressions in (9) and (10) we have $\xi_{ij}^A=m_{ij}\left(\cos(\phi_{ij}^A)(\boldsymbol{x}_{i1}-\boldsymbol{a}_{j1})+\sin(\phi_{ij}^A)(\boldsymbol{x}_{i2}-\boldsymbol{a}_{j2})\right)$, $\xi_{ik}^B=m_{ik}\left(\cos(\phi_{ik}^B)(\boldsymbol{x}_{i1}-\boldsymbol{x}_{k1})+\sin(\phi_{ik}^B)(\boldsymbol{x}_{i2}-\boldsymbol{x}_{k2})\right)$.

Similarly, from (11) and (12), we have $\zeta_{ij}^A=v_{ij}\sin\varphi_{ij}^A||\boldsymbol{x}_i-\boldsymbol{a}_j||$, $\zeta_{ik}^B=v_{ik}\sin\varphi_{ik}^B||\boldsymbol{x}_i-\boldsymbol{x}_k||$.

We define a vector $\boldsymbol{y}=[\boldsymbol{x}_1^T,\ \boldsymbol{x}_2^T,\ \ldots\ldots,\ \boldsymbol{x}_M^T]^T$ ($\boldsymbol{y}\in\mathbb{R}^{3M\times 1}$) as a column vector including all target locations, then $\boldsymbol{x}_i=\boldsymbol{E}_i^T\boldsymbol{y}$, where $\boldsymbol{E}_i=\boldsymbol{e}_i\otimes\boldsymbol{I}_3$, $\boldsymbol{e}_i$ denotes the ith column of the M-dimensional identity matrix, and $\otimes$ denotes Kronecker product.

According to LS criterion, the joint estimation of unknown parameters of $\boldsymbol{x}$ and η can be formulated as follows:

$$
\begin{aligned}
[\hat{\boldsymbol{y}},\hat{\eta}]=\arg\min_{\boldsymbol{y},\eta}\sum_A&\left[\frac{\mu^{-1}\left(\eta d_0^2-\left(\beta_{ij}^A\right)^2||\boldsymbol{E}_i^T\boldsymbol{y}-\boldsymbol{a}_j||^2\right)}{2\eta}\right]^2+\sum_A\left[\boldsymbol{c}_{ij}^T\left(\boldsymbol{E}_i^T\boldsymbol{y}-\boldsymbol{a}_j\right)\right]^2\\
&+\sum_A\left[\cos^2\left(\varphi_{ij}^A\right)||\boldsymbol{E}_i^T\boldsymbol{y}-\boldsymbol{a}_j||^2-\boldsymbol{k}^T\left(\boldsymbol{E}_i^T\boldsymbol{y}-\boldsymbol{a}_j\right)\left(\boldsymbol{E}_i^T\boldsymbol{y}-\boldsymbol{a}_j\right)^T\boldsymbol{k}\right]^2\\
&+\sum_B\left[\frac{\mu^{-1}\left(\eta d_0^2-(\beta_{ik}^B)^2||\boldsymbol{E}_i^T\boldsymbol{y}-\boldsymbol{E}_k^T\boldsymbol{y}||^2\right)}{2\eta}\right]^2+\sum_B\left[\boldsymbol{c}_{ik}^T\left(\boldsymbol{E}_i^T\boldsymbol{y}-\boldsymbol{E}_k^T\boldsymbol{y}\right)\right]^2\\
&+\sum_B\left[\cos^2\left(\varphi_{ik}^B\right)||\boldsymbol{E}_i^T\boldsymbol{y}-\boldsymbol{E}_k^T\boldsymbol{y}||^2-\boldsymbol{k}^T\left(\boldsymbol{E}_i^T\boldsymbol{y}-\boldsymbol{E}_k^T\boldsymbol{y}\right)\left(\boldsymbol{E}_i^T\boldsymbol{y}-\boldsymbol{E}_k^T\boldsymbol{y}\right)^T\boldsymbol{k}\right]^2.
\end{aligned}
\tag{13}
$$

2.1. Noncooperative Localization. In the noncooperative localization scenario, there is no communication link between target and target, so the set B in models (1)–(6) is empty. For ease of understanding, we just consider one target, i.e., $M=1$. In this case, (13) can be rewritten as follows:

$$
\begin{aligned}
\min_{\boldsymbol{x},\eta}\sum_{j=1}^N&\left(\frac{\mu^{-1}\left(\eta d_0^2-\beta_j^2||\boldsymbol{x}-\boldsymbol{a}_j||^2\right)}{2\eta}\right)^2+\sum_{j=1}^N\left(\boldsymbol{c}_j^T\left(\boldsymbol{x}-\boldsymbol{a}_j\right)\right)^2\\
&+\sum_{j=1}^N\left(\frac{\boldsymbol{k}^T\left(\boldsymbol{x}-\boldsymbol{a}_j\right)-\cos\varphi_j||\boldsymbol{x}-\boldsymbol{a}_j||}{\sin\varphi_j||\boldsymbol{x}-\boldsymbol{a}_j||}\right)^2.
\end{aligned}
\tag{14}
$$

Since (14) is a nonconvex problem, and it is difficult to obtain its solution directly. In the following section, we develop methods to transform this problem into a convex optimization problem by applying some relaxation techniques. For this purpose, we introduce auxiliary variable $\boldsymbol{h},\boldsymbol{f}$, and $\boldsymbol{g}$, where $\boldsymbol{f}_j=\boldsymbol{c}_j^T(\boldsymbol{x}-\boldsymbol{a}_j)$, then (14) can be expressed as follows:

$$
\begin{aligned}
\min_{\boldsymbol{x},\eta,\boldsymbol{h},\boldsymbol{f},\boldsymbol{g}}\ &\sum_{j=1}^N\boldsymbol{h}_j+||\boldsymbol{f}||^2+\sum_{j=1}^N\boldsymbol{g}_i\\
\text{s.t.}\ &\left\|\begin{bmatrix}2\mu^{-1}\left(\eta d_0^2-\beta_j^2||\boldsymbol{x}-\boldsymbol{a}_j||^2\right)\\ \eta^2\sigma_{n_j}^2-\boldsymbol{h}_j\end{bmatrix}\right\|\le\eta^2\sigma_{n_j}^2+\boldsymbol{h}_j\\
&\boldsymbol{f}_j=\boldsymbol{c}_j^T\left(\boldsymbol{x}-\boldsymbol{a}_j\right)\\
&\left\|\begin{bmatrix}2\left(\boldsymbol{k}^T\left(\boldsymbol{x}-\boldsymbol{a}_j\right)-\cos\varphi_j||\boldsymbol{x}-\boldsymbol{a}_j||\right)\\ \sin^2(\varphi_j)||\boldsymbol{x}-\boldsymbol{a}_j||^2-\boldsymbol{g}_j\end{bmatrix}\right\|\le\sin^2(\varphi_j)||\boldsymbol{x}-\boldsymbol{a}_j||^2+\boldsymbol{g}_j.
\end{aligned}
\tag{15}
$$

Furthermore, we introduce auxiliary variables $\boldsymbol{l}$ and $\boldsymbol{d}$, where $\boldsymbol{l}_j=||\boldsymbol{x}-\boldsymbol{a}_j||^2$ and $\boldsymbol{d}_j=||\boldsymbol{x}-\boldsymbol{a}_j||$, then problem (15) is equivalent to the following problem:

$$
\begin{aligned}
\min_{\substack{\boldsymbol{x},\eta,\boldsymbol{h},\boldsymbol{f},\boldsymbol{g}\\ \boldsymbol{l},\boldsymbol{d},t}}\ &\sum_{j=1}^N\boldsymbol{h}_i+t+\sum_{j=1}^N\boldsymbol{g}_i\\
\text{s.t.}\ &\left\|\begin{bmatrix}2\mu^{-1}\left(\eta d_0^2-\beta_j^2\boldsymbol{l}_j\right)\\ \eta^2\sigma_{n_j}^2-\boldsymbol{h}_j\end{bmatrix}\right\|\le\eta^2\sigma_{n_j}^2+\boldsymbol{h}_j\\
&\boldsymbol{l}_j=\boldsymbol{x}^T\boldsymbol{x}-2\boldsymbol{x}^T\boldsymbol{a}_j+||\boldsymbol{a}_j||^2\\
&\boldsymbol{f}_j=\boldsymbol{c}_j^T\left(\boldsymbol{x}-\boldsymbol{a}_j\right)\\
&\left\|\begin{bmatrix}2\left(\boldsymbol{k}^T\left(\boldsymbol{x}-\boldsymbol{a}_j\right)-\cos\varphi_j\boldsymbol{d}_j\right)\\ \sin^2(\varphi_j)\boldsymbol{l}_j-\boldsymbol{g}_j\end{bmatrix}\right\|\le\sin^2(\varphi_j)\boldsymbol{l}_j+\boldsymbol{g}_j\\
&\boldsymbol{d}_j=||\boldsymbol{x}-\boldsymbol{a}_j||\\
&||\boldsymbol{f}||^2\le t.
\end{aligned}
\tag{16}
$$

Next, we relax $z=\boldsymbol{x}^T\boldsymbol{x}$ into $z\ge\boldsymbol{x}^T\boldsymbol{x}$, which can be transformed into a linear matrix inequality, i.e., $\begin{bmatrix}\boldsymbol{I}_3 & \boldsymbol{x}\\ \boldsymbol{x}^T & z\end{bmatrix}\succeq 0$ by Schur complement [18], $\tau=\eta^2$ is transform into $\eta^2\le\tau$, additionally, $\boldsymbol{d}_j=||\boldsymbol{x}-\boldsymbol{a}_j||$ is transformed into $||\boldsymbol{x}-\boldsymbol{a}_j||\le\boldsymbol{d}_j$ by second-order cone relaxation (SOCR) technique.

Then, the final optimal problem can be written as follows:

$$
\begin{aligned}
\min_{\substack{\boldsymbol{x},\eta,\boldsymbol{h},\boldsymbol{f},\boldsymbol{g}\\ z,\boldsymbol{l},\boldsymbol{d},t,\tau}}\ &\sum_{j=1}^N\boldsymbol{h}_j+t+\sum_{j=1}^N\boldsymbol{g}_j\\
\text{s.t.}\ &\left\|\begin{bmatrix}2\mu^{-1}\left(\eta d_0^2-\beta_j^2\boldsymbol{l}_j\right)\\ \eta^2\sigma_{n_j}^2-\boldsymbol{h}_j\end{bmatrix}\right\|\le\eta^2\sigma_{n_j}^2+\boldsymbol{h}_j\\
&\boldsymbol{l}_j=z-2\boldsymbol{x}^T\boldsymbol{a}_j+||\boldsymbol{a}_j||^2\\
&\boldsymbol{f}_j=\boldsymbol{c}_j^T\left(\boldsymbol{x}-\boldsymbol{a}_j\right)\\
&\left\|\begin{bmatrix}2\left(\boldsymbol{k}^T\left(\boldsymbol{x}-\boldsymbol{a}_j\right)-\cos\varphi_j\boldsymbol{d}_j\right)\\ \sin^2(\varphi_i)\boldsymbol{l}_i-\boldsymbol{g}_i\end{bmatrix}\right\|\le\sin^2(\varphi_j)\boldsymbol{l}_j+\boldsymbol{g}_j\\
&||\boldsymbol{x}-\boldsymbol{a}_j||\le\boldsymbol{d}_j\\
&\left\|\begin{bmatrix}2\boldsymbol{f}\\ t-1\end{bmatrix}\right\|\le t+1,\quad\left\|\begin{bmatrix}2\eta\\ \tau-1\end{bmatrix}\right\|\le\tau+1\\
&\begin{bmatrix}\boldsymbol{I}_3 & \boldsymbol{x}\\ \boldsymbol{x}^T & z\end{bmatrix}\succeq 0.
\end{aligned}
\tag{17}
$$

The above is the proposed mixed SDP/second-order cone programing (SOCP) algorithm for noncooperative localization. This mixed SDP/SOCP algorithm is referred to as SDP/SOCP1.

2.2. Cooperative Localization. In the cooperative localization, we introduce variables $\boldsymbol{f}, \boldsymbol{g}, \boldsymbol{f}', \boldsymbol{g}'$, then (13) is equivalent to the following:

$$\begin{aligned}
\min_{y,\eta,f,g,f',g'} \; & \sum_A \left[\frac{\mu^{-1}\left(\eta d_0^2 - \left(\beta_{ij}^A\right)^2 ||\boldsymbol{E}_i^T \boldsymbol{y} - \boldsymbol{a}_j||^2\right)}{2\eta}\right]^2 \\
& + \sum_A \boldsymbol{f}_{ij}^2 + \sum_A \boldsymbol{g}_{ij}^2 \\
& + \sum_B \left[\frac{\mu^{-1}\left(\eta d_0^2 - \left(\beta_{ik}^B\right)^2 ||\boldsymbol{E}_i^T \boldsymbol{y} - \boldsymbol{E}_k^T \boldsymbol{y}||^2\right)}{2\eta}\right]^2 \\
& + \sum_B \boldsymbol{f}_{ik}'^2 + \sum_B \boldsymbol{g}_{ik}'^2 \\
\text{s.t.} \quad & \boldsymbol{f}_{ij} = \boldsymbol{c}_{ij}^T\left(\boldsymbol{E}_i^T \boldsymbol{y} - \boldsymbol{a}_j\right) \\
& \boldsymbol{g}_{ij} = \cos^2\left(\varphi_{ij}^A\right) ||\boldsymbol{E}_i^T \boldsymbol{y} - \boldsymbol{a}_j||^2 - \boldsymbol{k}^T\left(\boldsymbol{E}_i^T \boldsymbol{y} - \boldsymbol{a}_j\right)\left(\boldsymbol{E}_i^T \boldsymbol{y} - \boldsymbol{a}_j\right)^T \boldsymbol{k} \\
& \boldsymbol{f}_{ik}' = c_{ik}^T\left(\boldsymbol{E}_i^T \boldsymbol{y} - \boldsymbol{E}_k^T \boldsymbol{y}\right) \\
& \boldsymbol{g}_{ik}' = \cos^2\left(\varphi_{ik}^B\right) ||\boldsymbol{x}_i - \boldsymbol{x}_k||^2 - \boldsymbol{k}^T(\boldsymbol{x}_i - \boldsymbol{x}_k)(\boldsymbol{x}_i - \boldsymbol{x}_k)^T \boldsymbol{k}.
\end{aligned} \tag{18}$$

For the sake of ease, we stack the variables $\boldsymbol{f}_{ij}, \boldsymbol{g}_{ij}, \boldsymbol{f}_{ik}', \boldsymbol{g}_{ik}'$ into vector $\boldsymbol{z}$. And we introduce variables $\boldsymbol{h}, \boldsymbol{e}, t, \boldsymbol{d}_{ij}^{\mathrm{A}}, \boldsymbol{d}_{ik}^{\mathrm{B}}, \boldsymbol{Y}$, where $\boldsymbol{d}_{ij}^{\mathrm{A}} = ||\boldsymbol{E}_i^T \boldsymbol{y} - \boldsymbol{a}_j||^2, \boldsymbol{d}_{ik}^{\mathrm{B}} = ||\boldsymbol{E}_i^T \boldsymbol{y} - \boldsymbol{E}_k^T \boldsymbol{y}||^2, \; \boldsymbol{Y} = \boldsymbol{y}\boldsymbol{y}^T$. Then (18) is equivalent to the following:

$$\begin{aligned}
\min_{\substack{Y,y,\eta,h,e,t,\\ z,d_{ij}^A,d_{ik}^B}} \; & \sum_A \boldsymbol{h}_{ij} + \sum_B \boldsymbol{e}_{ik} + t \\
\text{s.t.} \quad & \left\| \begin{bmatrix} \mu^{-1}\left(\eta d_0^2 - \left(\beta_{ij}^A\right)^2 \boldsymbol{d}_{ij}^A\right) \\ \eta^2 - \boldsymbol{h}_{ij} \end{bmatrix} \right\| \le \eta^2 + \boldsymbol{h}_{ij} \\
& \boldsymbol{d}_{ij}^A = \operatorname{trace}(\boldsymbol{E}_i^T \boldsymbol{Y} \boldsymbol{E}_i) - 2\boldsymbol{a}_j^T \boldsymbol{E}_i^T \boldsymbol{y} + ||\boldsymbol{a}_j||^2 \\
& \left\| \begin{bmatrix} \mu^{-1}\left(\eta d_0^2 - \left(\beta_{ik}^B\right)^2 \boldsymbol{d}_{ik}^B\right) \\ \eta^2 - g_{ik} \end{bmatrix} \right\| \le \eta^2 + \boldsymbol{g}_{ik} \\
& \boldsymbol{d}_{ik}^B = \operatorname{trace}(\boldsymbol{E}_i^T \boldsymbol{Y} \boldsymbol{E}_i) - 2\operatorname{trace}(\boldsymbol{E}_i^T \boldsymbol{Y} \boldsymbol{E}_k) + \operatorname{trace}\left(\boldsymbol{E}_k^T \boldsymbol{Y} \boldsymbol{E}_k\right) \\
& \left\| \begin{bmatrix} \boldsymbol{z} \\ t - 1/4 \end{bmatrix} \right\| \le t + 1/4 \\
& \boldsymbol{Y} = \boldsymbol{y}\boldsymbol{y}^T.
\end{aligned} \tag{19}$$

The following optimization problems are formed by using techniques similar to the problem formation of (17), we relax $\boldsymbol{Y} = \boldsymbol{y}\boldsymbol{y}^T$ into $\boldsymbol{Y} \ge \boldsymbol{y}\boldsymbol{y}^T$, and $\tau = \eta^2$ into $\eta^2 \le \tau$.

$$\begin{aligned}
\min_{\substack{Y,y,\eta,h,e,t,\\ z,d_{ij}^A,d_{ik}^B,\tau}} \; & \sum_A \boldsymbol{h}_{ij} + \sum_B \boldsymbol{e}_{ik} + t \\
\text{s.t.} \quad & \left\| \begin{bmatrix} \mu^{-1}\left(\eta d_0^2 - \left(\beta_{ij}^A\right)^2 \boldsymbol{d}_{ij}^A\right) \\ \tau - \boldsymbol{h}_{ij} \end{bmatrix} \right\| \le \tau + \boldsymbol{h}_{ij} \\
& \boldsymbol{d}_{ij}^A = \operatorname{trace}(\boldsymbol{E}_i^T \boldsymbol{Y} \boldsymbol{E}_i) - 2\boldsymbol{a}_j^T \boldsymbol{E}_i^T \boldsymbol{y} + ||a_j||^2 \\
& \left\| \begin{bmatrix} \mu^{-1}\left(\eta d_0^2 - \left(\beta_{ik}^B\right)^2 \boldsymbol{d}_{ij}^B\right) \\ \tau - \boldsymbol{g}_{ik} \end{bmatrix} \right\| \le \tau + \boldsymbol{g}_{ik} \\
& \boldsymbol{d}_{ij}^B = \operatorname{trace}(\boldsymbol{E}_i^T \boldsymbol{Y} \boldsymbol{E}_i) - 2\operatorname{trace}(\boldsymbol{E}_i^T \boldsymbol{Y} \boldsymbol{E}_k) + \operatorname{trace}\left(\boldsymbol{E}_k^T \boldsymbol{Y} \boldsymbol{E}_k\right) \\
& \left\| \begin{bmatrix} \boldsymbol{z} \\ t - 1/4 \end{bmatrix} \right\| \le t + 1/4; \; \left\| \begin{bmatrix} \eta \\ \tau - 1/4 \end{bmatrix} \right\| \le \tau + 1/4; \; \begin{bmatrix} \boldsymbol{Y} & \boldsymbol{y} \\ \boldsymbol{y}^T & 1 \end{bmatrix} \ge 0.
\end{aligned} \tag{20}$$

The algorithm is referred to as SDP/SOCP2. SDP/SOCP1 and SDP/SOCP2 can be solved by CVX [24] in MATLAB.

3. Complexity Analysis

There exists a tradeoff between algorithm estimation accuracy and computational complexity, which is one of the most important indicators for evaluating the realizability of the algorithm. We analyze the worst-case complexity, i.e., we assume that the nodes in the network are interconnected, the total number of the communication link is $C = |A| + |B|$, where $|A| = MN, |B| = M(M-1)/2$. The formulation of hybrid SDP/SOCP in worst-case is shown as follows [19]:

$$O\left(\sqrt{\mu}\left(m\sum_{i=1}^{N_{sd}} n_i^{sd^3} + m^2\sum_{i=1}^{N_{sd}} n_i^{sd^2} + m^2\sum_{i=1}^{N_{soc}} n_i^{soc} + m^2\sum_{i=1}^{N_{soc}} n_i^{soc} + m^3\right)\right), \tag{21}$$

where m denotes the number of equation constraints, n_i^{sd} and n_i^{soc} denote the dimensions of ith semidefinite cone (SDC) and ith second-order cone (SOC), respectively. N^{sd} and N^{soc} denote the number of constraints of SDC and SOC, respectively, $\mu = \sum_{i=1}^{N_{sd}} n_i^{sd} + 2N_{soc}$ is the so-called barrier parameter. Since we investigate the worst-case complexity of the algorithm, the total number of communication links of the network is $K = |A| + |B|$, where $|A| = MN, |B| = M(M-1)/2$.

Based on (21), we calculate the complexity of the proposed and the existing algorithm in noncooperative and cooperative localization.

From Tables 1 and 2, we observe that the complexity of the algorithm is related to the number of sensors. Compared with noncooperative localization, the complexity of the cooperative localization is greatly higher.

4. CRLB

The CRLB is an unbiased estimation that can achieve the optimal estimation accuracy theoretically and can be used as a criterion for evaluating the performance of the localization algorithm. In the study of Kay [22], CRLB is expressed by the trace of F^{-1}, i.e.

Table 1: Summary of the considered method in noncooperative localization.

Method	Description	Complexity
WLS1	The WLS1 method by Tomic and Beko [20]	$O(N)$
GTRS1	The GTRS method by Qi et al. [15]	$2 \cdot O(K_{\max}N)$
SDP/SOCP1	The method proposed in Equation (17)	$O(N^{3.5})$

Table 2: Summary of the considered method in cooperative localization.

Method	Description	Complexity
SDP1	The SDP1 method used RSS measurement by Chang et al. [21]	$O(\sqrt{M}(4M^4(N+\frac{M}{2})^2))$
SDP2	The SDP2 method used hybrid RSS/AOA measurement by Qi et al. [15]	$O(\sqrt{3M}(81M^4(N+\frac{M}{2})^2))$
SDP/SOCP2	The method proposed in Equation (20)	$O(\sqrt{3M}(81M^4(N+2M)^2))$

$$\text{CRLB} = \text{trace}(F^{-1}), \tag{22}$$

where F denotes Fisher Information Matrix (FIM), in cooperative localization, we define a variable $\theta = [\boldsymbol{x}^T, \eta]$, the expression of FIM is shown as follows:

$$\mathscr{F}_{i,k} = E\left[\frac{\partial^2 \ln p(L;\theta)}{\partial\theta^2}\right], \tag{23}$$

where $p(L;\boldsymbol{x},L_0)$ is joint probability density function of the unknown parameter. F is as follows:

$$F = \begin{bmatrix} F_1 & F_2 \\ F_2^T & F_4 \end{bmatrix}, \tag{24}$$

where F_1 is a $3M \times 3M$ square matrix whose elements were given in [23], F2 and F4 are given as follows:

$$F_2 = \begin{bmatrix} \vdots \\ \sum_{\{j||(i,j)\in A\}} \xi \cdot \frac{\boldsymbol{x}_{i1} - \boldsymbol{s}_j}{||\boldsymbol{x}_i - \boldsymbol{s}_j||^2} + \sum_{\{k||(i,k)\in B\}} \xi \cdot \frac{\boldsymbol{x}_{i1} - \boldsymbol{x}_{k1}}{||\boldsymbol{x}_i - \boldsymbol{x}_k||^2} \\ \sum_{\{j||(i,j)\in A\}} \xi \cdot \frac{\boldsymbol{x}_{i2} - \boldsymbol{s}_j}{||\boldsymbol{x}_i - \boldsymbol{s}_j||^2} + \sum_{\{k||(i,k)\in B\}} \xi \cdot \frac{\boldsymbol{x}_{i2} - \boldsymbol{x}_{k2}}{||\boldsymbol{x}_i - \boldsymbol{x}_k||^2} \\ \sum_{\{j||(i,j)\in A\}} \xi \cdot \frac{\boldsymbol{x}_{i3} - \boldsymbol{s}_j}{||\boldsymbol{x}_i - \boldsymbol{s}_j||^2} + \sum_{\{k||(i,k)\in B\}} \xi \cdot \frac{\boldsymbol{x}_{i3} - \boldsymbol{x}_{k3}}{||\boldsymbol{x}_i - \boldsymbol{x}_k||^2} \\ \vdots \end{bmatrix},$$

$i = 1, \ldots, N$, $\xi = \frac{1}{\sigma_n^2} \cdot \frac{10\gamma}{\ln 10}$ and $F_4 = \sum_{\{j|\,|(i,j)\in A\}} \frac{1}{\sigma_n^2} + \sum_{\{k|\,|(i,k)\in B\}} \frac{1}{\sigma_n^2}$.

5. Results and Discussion

In this section, we compare the performance of the proposed algorithm with existing methods for both noncooperative and cooperative localization.

The normalized root mean square error (NRMSE) is introduced to evaluate localization performance, which is defined as follows:

$$\text{NRMSE}_{\boldsymbol{x}} = \sqrt{\frac{1}{M}\sum_{m=1}^{\text{Mc}}\sum_{i=1}^{M}\frac{\|\boldsymbol{x}_{im} - \widehat{\boldsymbol{x}}_{im}\|^2}{\text{Mc}}}, \tag{25}$$

and

$$\text{NRMSE}_{\text{TP}} = \sqrt{\frac{1}{M}\sum_{m=1}^{\text{Mc}}\frac{\left\|L_0 - \widehat{L}_0\right\|^2}{\text{Mc}}}, \tag{26}$$

where Mc denotes Monte Carlo (Mc) runs, M denotes the number of the targets, $\boldsymbol{x}_{i\,m}$ and $\widehat{\boldsymbol{x}}_{i\,m}$, respectively, denote true location and estimated location of the ith target in the mth MC run. Particularly, when $M = 1$, NRMSE is just RMSE (root mean square error).

We deploy N anchors and M targets randomly in a cube space $[0, 30] \times [0, 30] \times [0, 30]m^3$ in each Mc run. The reference distance is $d_0 = 1m$, the path loss exponent (PLE) is $\gamma = 2.5$. However, in practice, PLE is an experience value, which is closely related to the hardware condition and the wireless signal propagation environment, so PLE is assumed to follow the uniform distribution on an interval $[2.2, 2.8]$, i.e., $\gamma \in [2.2, 2.8]$.

5.1. Noncooperative Localization. In noncooperative WSN, targets communicate with anchors, exclusively. We compare the proposed algorithm with the previous algorithm, "WLS1," proposed by Yu [14], and "GTRS1," proposed by Tomic et al. [17]. For the sake of generality, we assume $M = 1$. In this part of simulation, $\text{Mc} = 5{,}000$.

Figure 2 shows the RMSE comparison of the proposed algorithm with the other methods versus the number of anchors when $\sigma_{n_i} = 6$ dB, $\sigma_{m_i} = 5$deg, $\sigma_{v_i} = 5$deg. Figure 2 shows that the localization performance becomes better as the number of anchors increases. This is due to the fact that more measurement information is utilized to estimate the target location. Furthermore, the estimation error of the proposed SDP/SOCP1 algorithm is smaller than that of and the proposed algorithm is closer to CRLB.

Figure 3 is the RMSE versus standard deviation of RSS measurement noise on target location estimation. Figure 3 shows that the localization performance of all the discussed

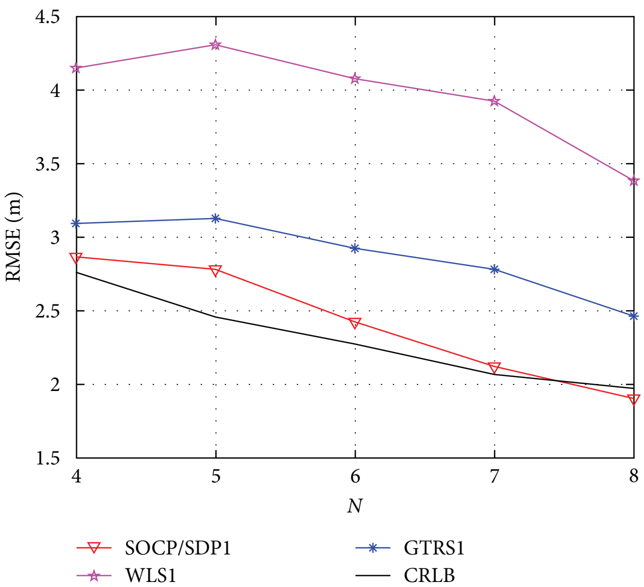

FIGURE 2: The RMSE of localization estimation versus N comparison.

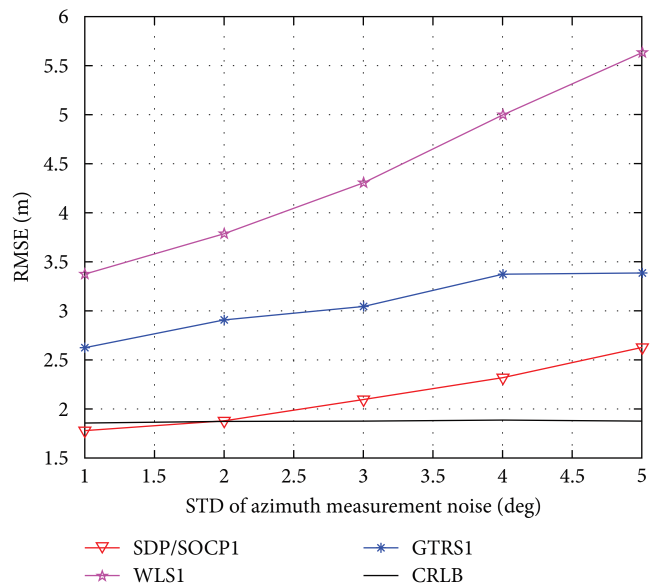

FIGURE 4: The RMSE-versus-σ_m comparison.

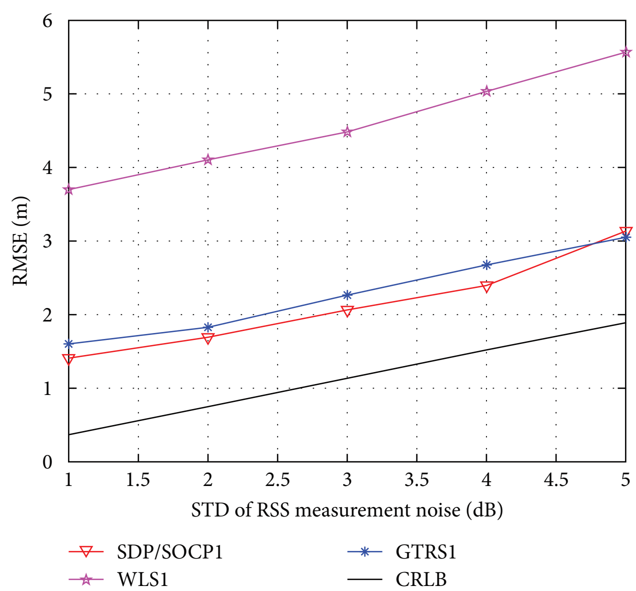

FIGURE 3: The RMSE-versus-σ_n comparison.

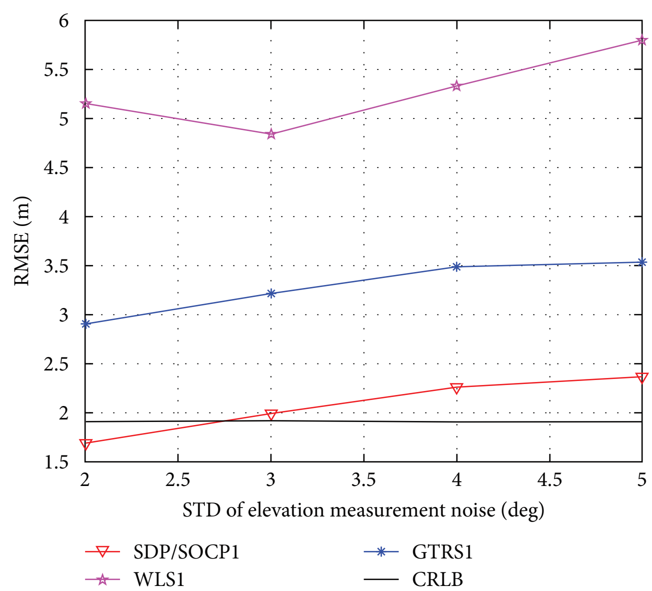

FIGURE 5: The RMSE-versus-σ_v comparison.

algorithms becomes worse as the quality of measurement weakens, as expected. Furthermore, the proposed algorithm provides the best performance among the discussed algorithms.

Figures 4 and 5 are the RMSE versus standard deviation of azimuth and elevation measurement noise on target location estimation, respectively. We get the similar conclusion as in Figure 3.

Figure 6 shows the RMSE comparison of the proposed algorithm with the others versus the number of anchors when $\sigma_{n_i} = 3$ dB, $\sigma_{m_i} = 3$deg, $\sigma_{v_i} = 3$deg. Figure 6 shows that the RMSE of the transmit power estimation is decrease as the number of anchors increases. Figure 6 also shows that the proposed algorithm provides the best estimation performance among the two discussed algorithms.

5.2. Cooperative Localization. Figure 7 shows the RMSE comparison of the methods versus the number of anchors when $\sigma_{n_i} = 5$ dB, $\sigma_{m_i} = 4$deg, $\sigma_{v_i} = 4$deg, $R = 8$ m. In the simulation, $\text{Mc} = 20{,}000$. Figure 7 shows that the NRMSE decreases as the number of nodes increases since more measurement information in target/target communication links can be captured to locate the target. Though the performance of the proposed algorithm is slightly better compared to SDP, it confirms that the localization performance of combined measurement in a hybrid system

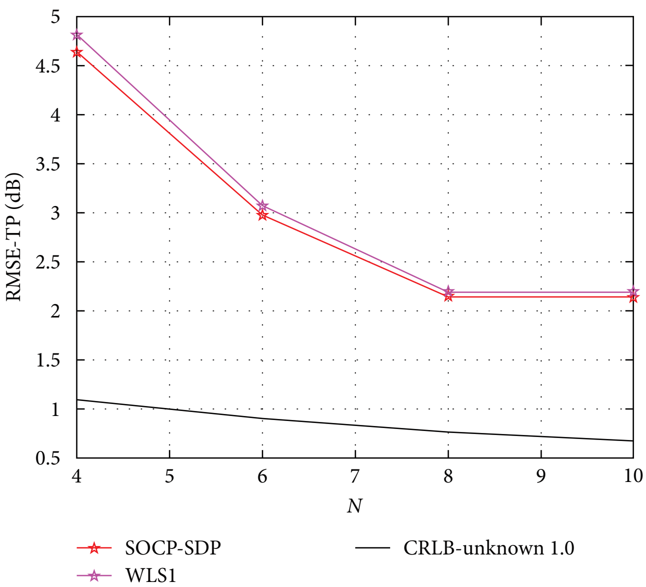

Figure 6: The RMSE of the transmit power estimation versus N comparison.

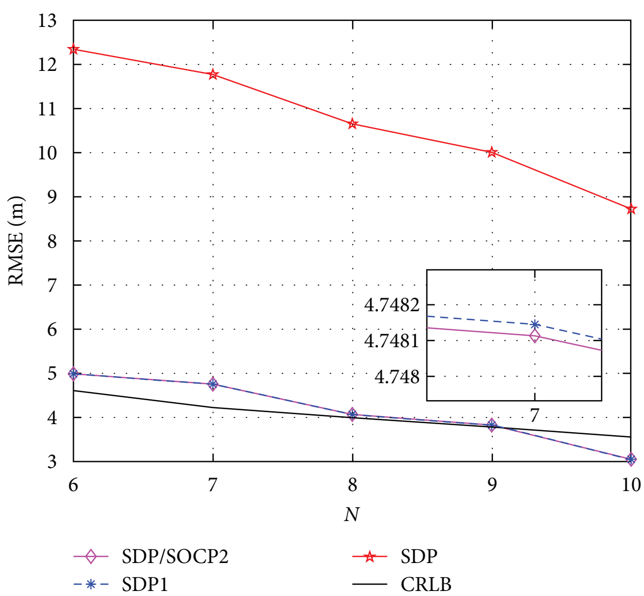

Figure 7: The RMSE-versus-M comparison.

is much better than single measurement in a traditional system.

6. Conclusions

In the paper, we have addressed the localization problem based on hybrid RSS–AOA measurement in noncooperative and cooperative scenarios when transmit power is unknown. Based on measurement model, we formulate original optimal problems according to LS criterion and transform the non-convex problem into mixed SDP/SOCP problems by some relaxation techniques, by means of which the unknown parameters $\boldsymbol{x}$ and η are jointly estimated.

We investigate the influence of a number of anchors and standard deviation of different types of measurement noise on localization accuracy in noncooperative localization scenarios; the results demonstrate the advantage of the proposed algorithm. Also, we investigate the influence of the number of targets on localization in a cooperative localization scenario; the results demonstrate that the performance of hybrid measurement is obviously better than a single measurement.

Data Availability

The data that support the findings of this study are available from the corresponding author upon reasonable request.

Conflicts of Interest

The authors declare that they have no conflicts of interest.

Acknowledgments

The authors would gratefully acknowledge the grants from the International Cooperation Pro-ject of the Ministry of Science and Technology under grant 2018YFE0206500, by the National Natural Science Foundation of China under grant 61571250, in part by the Zhejiang Natural Science Foundation under grant LY22F010018.

References

[1] H. Wymeersch, J. Lien, and M. Z. Win, “Cooperative localization in wireless networks,” *Proceedings of the IEEE*, vol. 97, no. 2, pp. 427–450, 2009.

[2] C. Tang, L. Zhang, Y. Zhang, and H. Song, “Factor graph-assisted distributed cooperative positioning algorithm in the GNSS system,” *Sensors*, vol. 18, no. 11, Article ID 3748, 2018.

[3] I. F. Akyildiz, W. Su, Y. Sankarasubramaniam, and E. Cayirci, “Wireless sensor networks: a survey,” *Computer Networks*, vol. 38, no. 4, pp. 393–422, 2002.

[4] S. Wu, S. Zhang, and D. Huang, “A TOA-based localization algorithm with simultaneous NLOS mitigation and synchronization error elimination,” *IEEE Sensors Letters*, vol. 3, no. 3, pp. 1–4, 2019.

[5] J. Shen, A. F. Molisch, and J. Salmi, “Accurate passive location estimation using TOA measurements,” *IEEE Transactions on Wireless Communications*, vol. 11, no. 6, pp. 2182–2192, 2012.

[6] K. W. K. Lui, W.-K. Ma, H.-C. So, and F. K. W. Chan, “Semi-definite programming algorithms for sensor network node localization with uncertainties in anchor positions and/or propagation speed,” *IEEE Transactions on Signal Processing*, vol. 57, no. 2, pp. 752–763, 2009.

[7] S. Chang, Y. Li, X. Yang, H. Wang, W. Hu, and Y. Wu, “A novel localization method based on RSS-AOA combined measurements by using polarized identity,” *IEEE Sensors Journal*, vol. 19, no. 4, pp. 1463–1470, 2019.

[8] J. Shi, G. Wang, and L. Jin, “Least squared relative error estimator for RSS based localization with unknown transmit power,” *IEEE Signal Processing Letters*, vol. 27, pp. 1165–1169, 2020.

[9] Y. Zheng, M. Sheng, J. Liu, and J. Li, “Exploiting AoA estimation accuracy for indoor localization: a weighted AoA-

based approach," *IEEE Wireless Communications Letters*, vol. 8, no. 1, pp. 65–68, 2019.

[10] D. J. An, C.-M. Moon, and J.-H. Lee, "Derivation of an explicit expression of an approximate location estimate in AOA-based localization," in *2017 7th IEEE International Symposium on Microwave, Antenna, Propagation, and EMC Technologies (MAPE)*, pp. 552–555, IEEE, Xi'an, China, 2017.

[11] Y. Wang and K. C. Ho, "Unified near-field and far-field localization for AOA and hybrid AOA-TDOA positionings," *IEEE Transactions on Wireless Communications*, vol. 17, no. 2, pp. 1242–1254, 2018.

[12] M. Katwe, P. Ghare, and P. K. Sharma, "Robust NLOS bias mitigation for hybrid RSS-TOA based source localization under unknown transmission parameters," *IEEE Wireless Communications Letters*, vol. 10, no. 3, pp. 542–546, 2021.

[13] S. Chang, Y. Zheng, P. An, J. Bao, and J. Li, "3-D RSS-AOA based target localization method in wireless sensor networks using convex relaxation," *IEEE Access*, vol. 8, pp. 106901–106909, 2020.

[14] K. Yu, "3-d localization error analysis in wireless networks," *IEEE Transactions on Wireless Communications*, vol. 6, no. 10, pp. 3472–3481, 2007.

[15] H. Qi, L. Mo, and X. Wu, "SDP relaxation methods for RSS/AOA-based localization in sensor networks," *IEEE Access*, vol. 8, pp. 55113–55124, 2020.

[16] S. Tomic, M. Beko, and M. Tuba, "A linear estimator for network localization using integrated RSS and AOA measurements," *IEEE Signal Processing Letters*, vol. 26, no. 3, pp. 405–409, 2019.

[17] S. Tomic, M. Beko, and R. Dinis, "3-D target localization in wireless sensor networks using RSS and AoA measurements," *IEEE Transactions on Vehicular Technology*, vol. 66, no. 4, pp. 3197–3210, 2017.

[18] S. Boyd and L. Vandenberghe, *Convex Optimization*, Cambridge University Press, 2004.

[19] I. Pólik and T. Terlaky, "Interior point methods for nonlinear optimization," in *Nonlinear Optimization*, vol. 1989 of *Lecture Notes in Mathematics*, pp. 215–276, Springer, Berlin, Heidelberg, 2010.

[20] S. Tomic and M. Beko, "A robust NLOS bias mitigation technique for RSS-TOA-based target localization," *IEEE Signal Processing Letters*, vol. 26, no. 1, pp. 64–68, 2019.

[21] S. Chang, Y. Li, H. Wang, W. Hu, and Y. Wu, "RSS-based cooperative localization in wireless sensor networks via second-order cone relaxation," *IEEE Access*, vol. 6, pp. 54097–54105, 2018.

[22] S. M. Kay, *Fundamentals of Statistical Signal Processing: Estimation Theory*, Prentice-Hall, Inc., 1993.

[23] Q. Qi, Y. Li, Y. Wu, Y. Wang, and Y. Yue, "RSS-AOA-based localization via mixed semi-definite and second-order cone relaxation in 3-D wireless sensor networks," *IEEE Access*, vol. 7, pp. 117768–117779, 2019.

[24] M. Grant, S. Boyd, and Y. Ye, "CVX users' guide," Tech. Rep. Build. Cambridge Univ. 711, 2009.